J Solid State Electrochem (2012) 16:3457–3465
DOI 10.1007/s10008-012-1909-y

ORIGINAL PAPER

# Effect of nano-$Al_2O_3$ particles and of the Co concentration on the corrosion behavior of electrodeposited Ni–Co alloys

**Geta Cârâc · Adriana Ispas**

Received: 6 June 2012 / Revised: 4 October 2012 / Accepted: 7 October 2012 / Published online: 25 October 2012
© Springer-Verlag Berlin Heidelberg 2012

**Abstract** Incorporation of nano-$Al_2O_3$ particles into a Ni–Co alloy by electrodeposition influences the corrosion properties, morphology, and structure of the layers. The resistance against corrosion of Ni–Co/$Al_2O_3$ composite films deposited on stainless steel was investigated in a 0.1-M NaCl solution by potentiodynamic polarization. The presence of nanoparticles improves the corrosion resistance of Ni–Co/nano-$Al_2O_3$ deposits when compared to pure Ni–Co alloy. Moreover, by increasing the pH of the electrodeposition bath and the content of Co in the alloy, the resistance against corrosion is furthermore improved. The morphology of the deposits before and after their corrosion was analyzed by scanning electron microscopy. The presence of the embedded alumina particles in the Ni–Co alloys was one of the key factors that limited further propagation of corrosion on the metallic surface. Preferential corrosion attack, in the form of a pitting corrosion, was located mainly at the grain boundaries.

**Keywords** Ni–Co alloys · Alumina nanoparticles · Potentiodynamic polarization · Corrosion · Electrodeposition

G. Cârâc (✉)
Department of Chemistry, Physics and Environment, Faculty of Sciences and Environment, "Dunarea de Jos" University of Galati, Domneasca 47 Street,
800008 Galati, Romania
e-mail: getac@ugal.ro

A. Ispas
Fachgebiet Elektrochemie und Galvanotechnik II,
Technische Universität Ilmenau,
Gustav-Kirchhoff-Straße 6,
98693 Ilmenau, Germany

## Introduction

The metallic alloys obtained by electrochemical or metallurgical procedures are important for different technological applications [1, 2]. The Ni–Co alloy thin films are used in various magnetic devices, especially in the technology of micro-systems, in manufacturing sensors, actuators, and memory devices [3, 4]. However, cobalt is expensive and drastically increases the total cost for alloys. Therefore, some works have been carried out in order to reduce its content in the deposits. Different proportions of these two metals can be obtained by using variable deposition parameters, but for all $Ni^{2+}/Co^{2+}$ ratios studied, preferential deposition of cobalt occurs and anomalous codeposition takes places [5, 6]. The anomalous Ni–Co codeposition was explained by several mechanisms, in different studies [7–10]. Thus, it can occur due to an increase of pH near the electrode surface, and therefore, cobalt hydroxide will precipitate on the surface. According to a two-step reduction mechanism, the anomalous codeposition consists of a competitive adsorption of a monovalent intermediate followed by its reduction to the elemental state. Anomalous codeposition may also be due to underpotential deposition and faster kinetics of cobalt species [7–10].

The development of science and technology requires improving the coating performance in order to reach higher standards. The actual research focuses on electrodeposition of composite coatings which present enhanced mechanical properties (wear resistance, hardness, and abrasion) and better corrosion resistance than the pure matrix. An important question at which no general answer has been found yet is to determine the mechanism that governs the embedding of nano-sized ceramic particles in a metallic matrix. Still there is no general theory that describes how one can obtain a uniform distribution of the nanoparticles in a metallic

matrix, as well as the relation between the concentration of particles that are dispersed in the electrolyte, and the amount one can find incorporated in the deposits [6].

The composite coatings based on Ni–Co alloys can be used in many industrial fields. For example, the codeposition of Ni–Co alloys with alumina or chromium carbide particles is interesting in building aerospace components, due to their resistance against oxidation at high temperatures [11, 12]. So far, the effects of the different fabrication techniques on the microstructure and properties of the thin films of $Al_2O_3$ nanoparticles (n-$Al_2O_3$) in a Ni–Co matrix were studied [13–16]. The composite coatings which contained nanoparticles exhibited a higher hardness, higher temperature resistance, and smaller grain size among other properties, which makes them more interesting for possible industrial application than the pure alloys. Therefore, due to their superior mechanical properties and corrosion protection, the Ni–Co alloys reinforced with oxide or magnetic nanoparticles have been the subject of various investigations [16–19]. Simultaneously, these studies tried to gain insight into the fundamental mechanisms which control the physical properties of the codeposition process.

Scarce literature studies discuss the corrosion behavior of Ni–Co/n-$Al_2O_3$ thin layers. Our work intends to bring more light on this matter. In this study, we report on the effect of incorporation $Al_2O_3$ nanoparticles in a Ni–Co matrix on the corrosion resistance and microstructure of the films. The advantages of oxide particles incorporation, as well as the reason why Ni–Co alloys are interesting systems due to their chemical, physical, and mechanical properties, will be also discussed.

## Experimental

### Electrodeposition process

Nickel–cobalt alloys and Ni–Co/n-$Al_2O_3$ composite coatings were electrodeposited from a Watts-type electrolyte containing different concentrations of Co ions and nano-$Al_2O_3$ particles. All electrochemical experiments were performed by using direct current in a three-electrode cell under mechanical stirring (700 rpm). The composition of electrolyte and the working parameters are shown in Table 1. The electrolyte was freshly prepared by dissolving reagent-grade chemicals in double-distilled water. All electrodeposition experiments of alloys and composite coatings were carried out using a PS6 Potentiostat from Meinsberg GmbH. The working electrode was a stainless steel plate with an active surface area of 25 $cm^2$ and a nickel plate was used as counter electrode. The counter electrode was approximately two times larger than the working electrode. A saturated calomel electrode (SCE) was used as reference electrode. The

**Table 1** Overview of the electrodeposition parameters

| Electrolyte composition | The working parameters |
|---|---|
| 0.90 M $NiSO_4 \cdot 6H_2O$ | Current density, 2 $A dm^{-2}$ |
| 0.21 M $NiCl_2 \cdot 6H_2O$ | Deposition time, 60 min |
| 0.48 M $H_3BO_3$ | Temperature, 50 °C |
| $10^{-4}$M dodecyl sodium sulfate | Stirring rate, 700 rpm |
| $CoSO_4 \cdot 7H_2O$, 35.6 and 106.7 mM | Working electrode surface area, 25 $cm^2$ |
| pH4–4.2 | Nano-$Al_2O_3$, 5 and 10 $g dm^{-3}$ |

concentration in nickel ions of the electrolytes was kept constant around 0.1 $mol dm^{-3}$. Two ratios for molarity of $Ni^{2+}$/$Co^{2+}$ ions in the electrolyte were investigated (1:1 and 3:1).

The stainless steel substrates were immersed in the electrolyte after they were polished and chemical activated in 1 M HCl solution. The deposition time was chosen to be 60 min and the current density was 2 $A dm^{-2}$. The electrolyte pH was carefully controlled during the entire time when the deposition took place, and it was adjusted at a value between 4 and 4.2 with suitable additions of diluted $H_2SO_4$ solution. All investigations were performed at a temperature of 50 °C, similar to the conditions used in an industrial process. The nanoparticles of $Al_2O_3$ were bought from Degussa. They had an average primary size of 20 nm, and they were added to the electrolyte in two different concentrations (5 and 10 $g dm^{-3}$). The electrolyte-containing nanoparticles were stirred mechanically for 24 h prior to deposition experiments. Before the measurements, the electrolytes were purged for 5 min by nitrogen bubbling, in order to reduce the amount of dissolved oxygen.

The average thickness of the deposited layers was 30.5± 6 μm for Ni–Co alloys and 54.2±8 μm for Ni–Co/n-$Al_2O_3$ composite coatings, respectively. The thickness of the layers was determined based on the mass deposited (which was obtained by weighting the samples before and after deposition experiments), considering the active geometrical area of the working electrode and the density of the deposits. The density of the deposits was calculated for each individual sample based on its composition. The standard deviations from four measurements are given above as the error obtained when determining the thickness of the layers. Stirring the solution during the electrodeposition helped in obtaining deposits with a uniform distribution of the $Al_2O_3$ nanoparticles, but also minimized the locally increasing pH in front of the working electrode.

### Corrosion measurements

The corrosion tests (in form of potentiodynamic polarization) of the electrodeposited coatings were carried out at 25 °C in 0.1 M NaCl electrolyte, at different times after their immersion

in this test solution, working with a three-electrode configuration electrochemical cell. Defined areas of 0.13 $cm^2$ and of 0.28 $cm^2$ from the deposits were exposed to the electrolyte. A Pt plate was used as counter electrode and an SCE was used as reference electrode. The SCE was placed inside a Luggin capillary, and thus, it was brought near the vicinity of the working electrode, in order to minimize the solution resistance. All electrode potentials presented in the following figures refer to the standard SCE. A PS6 Potentiostat from Meinsberg GmbH was used in the corrosion tests.

Four identical experiments for each sample were performed in our study, in different areas of the surface. The potential was swept from −500 to +400 mV (in some experiments also up +1.400 V or even to +2.000 V), at a scan rate of 0.5 $mV\,s^{-1}$. The potential scan was initiated all the time in the negative direction.

### Analysis of morphology, composition, and structure of the layers

The microstructure of alloys and of composite coatings before and after corrosion tests was analyzed with a scanning electron microscope (SEM from Zeiss, type LEO 1455 VP, equipped with an energy-dispersive X-ray (EDX) detector). Simultaneous to SEM measurements, EDX analyses were performed for each deposit, in order to check the composition of the alloys and composite coatings. The volume fraction of $Al_2O_3$ nanoparticles that were embedded in the Ni–Co alloy matrix was calculated using the EDX data. X-ray diffractometer (D5000 from Siemens) with $CoK_\alpha$ radiation was used for detecting the structure of the deposits.

## Results and discussion

### Codeposition of nano-$Al_2O_3$ into Ni–Co alloy matrix

Many factors contribute to the quality of the electrodeposited coatings. The effect of nano-particles on the corrosion behavior as well as on the mechanical properties depends on the electrodeposition parameters. Previous observations indicate that the composition of the plating electrolyte has a strong influence on the layer composition, microstructure, and their corrosion protection, both for the Ni–Co alloys and Ni–Co/n-$Al_2O_3$ composite coatings [1–24]. Another important factor is the pH of the electrolyte. By controlling the pH value, one can control the deposition growth kinetics, chemical composition, and morphology of the films. In this study, we kept the pH value of the electrolyte constant, in order to minimize its influence on the film properties. Another factor that was taken into account in this study is the mechanical agitation of the electrolyte. The stirring of the electrolyte minimizes the inhibition process on embedding of particles in the metallic matrix, which was detected at high deposition rates. Moreover, a wider range of electrical potentials, at which the obtained deposits are uniform and fine grained, can be used if the electrolyte is mechanically stirred [20, 21]. The stirring of the bath chosen in this study (700 rpm) prevents both the strong depletion in $Co^{2+}$ (the electroactive species which is in lower concentration in electrolyte) in front of the working electrode and the sedimentation of nano-$Al_2O_3$ particles.

It is also desirable that the composition of the electrodeposited composite coatings and that of Co–Ni alloys remains constant throughout the entire thickness of the deposited films. In our study, the composition of Co–Ni alloy, as determined by EDX, was almost constant in the entire thickness of the deposits. The composition of the deposits was determined from cross section of some chosen samples and the values obtained are presented in Table 2, in weight percent, as the average of a minimum five different measurements. The standard error of the values obtained for the composition is also reported in Table 2. One can see in Table 2 that the amount of $Al_2O_3$ particles incorporated in the layer increases with an increase in the concentration of particles in the electrolyte. Moreover, the amount of $Co^{2+}$ present in the electrolyte seems to have a beneficial influence on the amount of incorporated nanoparticles.

When both nickel and cobalt ions are present in the bath, the nickel is always deposited first. However, the things can be completely different if complexes of Ni and Co are present in the electrolyte, as when the electrolyte contains just simple $Ni^{2+}$ and $Co^{2+}$ [24]. When some nickel is deposited on the electrode, $Co^{2+}$ species adsorb on the freshly electrodeposited nickel, hindering the normal nickel deposition, as it can be observed in the solutions with 0.1 M $NiCl_2$ and very low concentrations of $Co^{2+}$ ions [24]. In this case, the partial current due to cobalt deposition is quite low, but the final result is an inhibition of nickel deposition. The nano-$Al_2O_3$ added in the electrolyte did not change the anomalous codeposition behavior of $Co^{2+}$ into Ni–Co alloy matrix.

The alumina particles could be incorporated in the Co–Ni matrix via their adsorption on the cathode surface during electrocodeposition process. An increase of the percentage of $Al_2O_3$ particles that are incorporated in the films with an increase in the $Co^{2+}$ ion concentration in the electrolyte was observed. Thus, the $Co^{2+}$ ions contribute more than the $Ni^{2+}$ to the codeposition of $Al_2O_3$ particles probably due the stronger adsorption of $Co^{2+}$ ions on the particles surface. However, further increases in the alumina concentration in the baths could not be so beneficial, as a saturation level of the alumina adsorption on the cathode surface could be reached.

### Morphology and structure of the deposited layers

The SEM images of Ni–Co and Ni–Co/n-$Al_2O_3$ composite coatings prepared by electrodeposition are shown in Figs. 1

**Table 2** The composition of Ni–Co alloys and Ni–Co/n-$Al_2O_3$ composite coatings, as determined from EDX analysis

| Samples | $Ni^{2+}/Co^{2+}$ ratio in electrolyte | $Al_2O_3$ in electrolyte ($g\,dm^{-3}$) | Ni (wt%) | Co (wt%) | $Al_2O_3$ in deposits | |
|---|---|---|---|---|---|---|
| | | | | | (wt%) | (vol.%) |
| Ni–Co alloys | 3:1 | – | 78.9±0.9 | 21.1±1.1 | – | – |
| | 1:1 | – | 61.8±1.1 | 38.2±2.1 | – | – |
| Ni–Co/n-$Al_2O_3$ composite coatings | 3:1 | 5 | 77.5±2.1 | 20.6±0.8 | 1.9±0.3 | 2.3 |
| | | 10 | 68.2±1.7 | 26.6±1.3 | 5.2±0.6 | 6.5 |
| | 1:1 | 5 | 71.8±0.8 | 26.0±1.2 | 2.2±0.2 | 2.7 |
| | | 10 | 58.1±1.1 | 36.1±0.8 | 5.8±0.1 | 7.3 |

and 2, respectively, before and after the corrosion tests. The deposits' morphologies varied with the bath composition and the applied anodic potential limit for corrosion tests. Generally, the deposits obtained in this study exhibited a compact surface and fine grains. The nano-$Al_2O_3$ particles were homogeneously deposited onto the entire surface and inside the deposits.

The presence of cobalt ions drastically influences the morphology of the Ni–Co alloys. From the SEM images, it can be concluded that the morphological appearance of Ni–Co alloys changes with varying the $Co^{2+}$ concentration in the bath, passing from that of pure Ni to the microstructure of pure Co, as the Co content increases in the alloy.

Embedding of $Al_2O_3$ particles did not affect strongly the shiny visual macroscopic aspect of the deposits from a Watts bath. However, microscopically, one could see that the morphology of the deposits changes with an increase in the concentration of incorporated alumina particles. Thus, the surfaces of composites were smoother and with smaller crystalline grains than of the pure Ni–Co alloys. This fact can be explained by the specific distribution of nano-$Al_2O_3$ particles in the Ni–Co matrix, especially along the boundaries of metallic grains. The presence of alumina particles restricts the growth of Ni and Co grains during the electrodeposition and induces the formation of finer and more compact surfaces. More homogeneous, fine-grained deposits were obtained by increasing the $Ni^{2+}/Co^{2+}$ ratio in the solution.

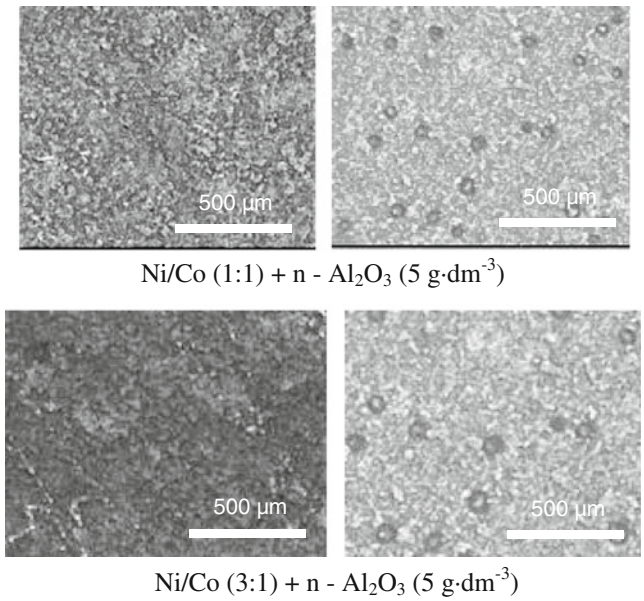


**Fig. 1** SEM images on Ni–Co/n-$Al_2O_3$ surfaces before (*left images*) and after (*right images*) the corrosion test

After their corrosion, the Ni–Co alloys tested in this study in 0.1 M NaCl solution presented large localized corrosion pits. The black regions in Figs. 1 and 2 represent the regions where the pitting corrosion was initiated. An interesting morphological feature of these pits is their almost perfect circular shape, a fact often reported when pitting corrosion occurs on different metal surfaces [25, 26]. The surfaces of the hemispherical pits will have a polished appearance if the pits grow under mass transport control, or they will present an irregular shape in case the process is mixed controlled or under charge transport control. One can see in Figs. 1 and 2 that in our case, the surface of the pits, which are represented by the darker regions in the SEM images, was not a polished one, which is proven by the presence of more white spots within the black regions. Therefore, based on the SEM observations and on the polarization curves (discussion in Section on Corrosion tests), one can conclude that in our case, the pitting corrosion was under mixed control.

The pitting corrosion was usually initiated on the surface between two globular structures. This can be better visualized in the case that layers were deposited from an electrolyte containing $Ni^{2+}/Co^{2+}$ in a concentration ratio of 1:1 and 10 $g\,dm^{-3}$ alumina nanoparticles (Fig. 2). Increasing the potential window for the corrosion tests induced the formation of larger pits. This can be explained on the basis of the different characteristic potentials that exist for a material that corrodes by pitting corrosion. Thus, stable pits will form at potentials noble to the critical pitting potential, while the pits will grow at potentials noble to the repassivation [25–27].

## Corrosion tests

The Ni–Co composite coatings cover themselves in atmosphere with a thin natural oxide film. The desired characteristics with

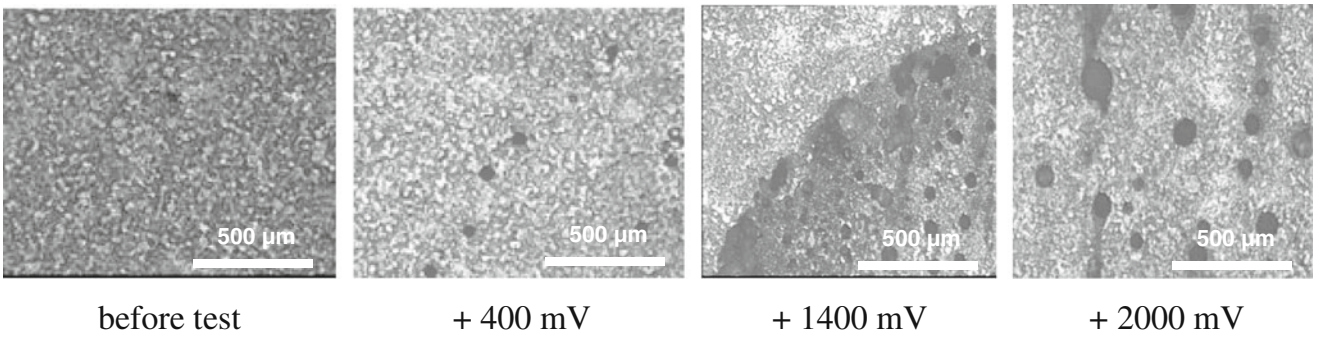


**Fig. 2** SEM images showing the corrosion evolution on surface of Ni–Co (1:1)+n-$Al_2O_3$ (10 $gdm^{-3}$) films after potentiodynamic polarization experiments with different anodic potentials limits

regard to corrosion protection of this formed oxide film are to be dense, well adhered to the metallic alloy, and insoluble in typical electrolyte media. However, in reality, this happens rarely, and the Ni and Ni-based alloys corrode in atmosphere and in electrolytes. Normally, the corrosion of metals in atmosphere takes place at a negligible corrosion rates when compared to the corrosion in electrolytes. Many studies have shown that the corrosion of Ni or the high Ni alloys at high temperature or when electrolytes are introduced under alternate oxidation/reduction states happens mainly along the grain boundaries [25, 27]. On another hand, most of the $Al_2O_3$ particles were usually found to be incorporated between the grains (see discussion in Section on Morphology and structure of the deposited layers). Therefore, it is interesting to study the corrosion behavior of the Ni–Co layers containing $Al_2O_3$ particles. Some of the obtained deposits (prepared by using a different $Ni^{2+}/Co^{2+}$ concentration ratio and a variable content of $Al_2O_3$ nanoparticles in the electrolyte, as described in Table 1) were selected for checking their corrosion behavior as a function of the incorporated amount of $Al_2O_3$ nanoparticles.

The first evaluation of the corrosion behavior for the Ni–Co alloys and the Ni–Co/n-$Al_2O_3$ composite coatings was done by recording the open circuit potential, OCP, values (vs. SCE) in 0.1 M NaCl solution, for 30 min. The obtained results are presented in Fig. 3 for two different defined areas on the samples. One can see in Fig. 3 that the OCP varied between −250 and ca. −370 mV vs. SCE. More cathodic OCP values were recorded for the larger sample area than for the smaller sample area for the pure alloys as well as for the Ni–Co/n-$Al_2O_3$ obtained from a bath containing 5 g $dm^{-3}$ $Al_2O_3$ nanoparticles. For the samples obtained in an electrolyte containing 10 $gdm^{-3}$ $Al_2O_3$ nanoparticles, the OCP values recorded for the smaller areas of the electrode were more cathodic than those recorded for the bigger areas of the electrode.

The dependence of the OCP values on the exposed areas of the electrode was not expected. Normally, the OCP values should be independent on the area exposed to the electrolyte, if the deposited layer is homogeneous. However, we obtained different OCP values for different areas exposed. This fact can be correlated to the pits formed by corrosion and also to the fact that the $Al_2O_3$ particles incorporated preferentially along the grain boundary influence the corrosion of the deposited films. As a final effect, on the area of the deposits over which oxidation or reductions occur, there will be a different ratio of anodic–cathodic sites. When the deposited layers are not homogeneous, this ratio can have different values as a function of the initial surface that is corroding. Of course, in this case, the OCP values will not be representative for the entire surface of the samples, but will be dependent solely on the area that is affected by the corrosion attack.

Incorporating more oxide particles in the deposited layers induces a higher resistance against the corrosion of these layers. A larger variation in the OCP (of about 100 mV) was observed for Ni–Co alloys obtained when $Ni^{2+}/Co^{2+}$ ratio in electrolyte was 1:1, when compared to the alloys obtained when the $Ni^{2+}/Co^{2+}$ ratio in electrolyte was 3:1 (ca. 50 mV).

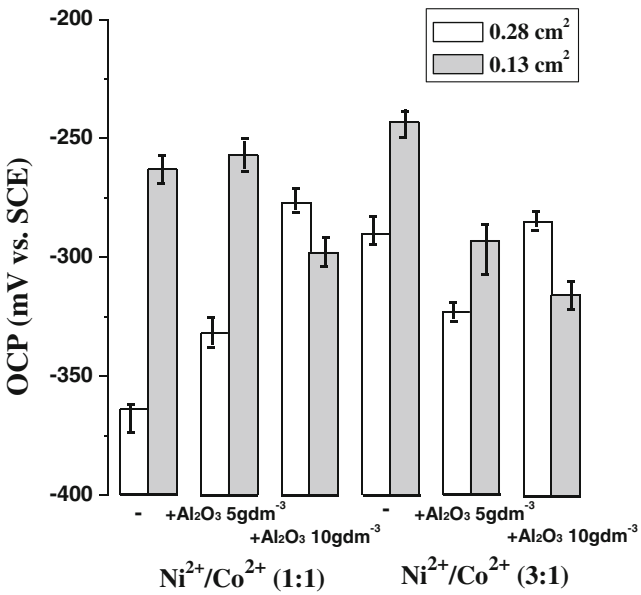


**Fig. 3** OCP values of Ni–Co and Ni–Co/n-$Al_2O_3$ layers recorded for 30 min on different defined surface areas exposed to 0.1 M NaCl solution

This fact can be correlated with the morphology of the samples (Figs. 1 and 2 and discussion in Section on Morphology and structure of the deposited layers). Thus, more homogeneous and less rough layers were obtained when the concentration ratio of $Ni^{2+}/Co^{2+}$ in the electrolyte was 3:1 than when it was 1:1. The low roughness induced the existence of less point defects where the pitting corrosion could start, and therefore, the differences obtained in the value of the OCP when one exposed larger or smaller area to the corrosion test solution were minimal in this case.

The OCP values of the layers deposited from a solution containing 1:1 $Ni^{2+}/Co^{2+}$ ion concentration ratio shifted gradually towards anodic potential range with an increase in the $Al_2O_3$ content, in the case that a bigger area of the electrode was exposed. However, the OCP goes more cathodic with an increase in the $Al_2O_3$ content when a smaller area of the electrode was exposed, for the layers obtained from a 3:1 $Ni^{2+}/Co^{2+}$ solution. In the other two cases shown in Fig. 3, no clear tendency of the OCP values as a function of the $Al_2O_3$ content was observed. The OCP tendencies mentioned above can be again correlated to the morphology of the deposited layers and to the existence of different ratio of anodic–cathodic corrosion sites on different areas exposed to corrosion. Thus, smoother surfaces presented an increased corrosion resistance than the rougher surfaces. At the same time, the presence of alumina particles proved to be beneficial for improving the uniformity of the layers on larger areas when an electrolyte diluted in $Co^{2+}$ ions was used. However, on smaller areas, it reduced the resistance to the corrosion of the layers deposited from both electrolytes, containing 1:1 or 3:1 $Ni^{2+}/Co^{2+}$ ion concentration.

Linear potential sweeps were also performed in order to get more information on the corrosion behavior of the deposits. The polarization diagrams as well as the values of corrosion potentials and the corrosion currents that were thus obtained are presented in Figs. 4, 5, 6, and 7 and in Table 3. The $j_{corr}$ was determined from the intersection of the polarization curves associated to the anodic and cathodic partial reactions.

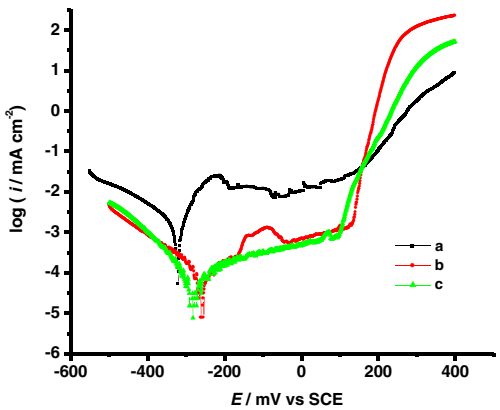


**Fig. 4** Potentiodynamic curves in 0.1 M NaCl for Ni–Co alloys: **a** pure Ni; **b** Ni–Co (1:1); **c** Ni–Co (3:1). Scan rate 0.5 $mV s^{-1}$; 25 °C

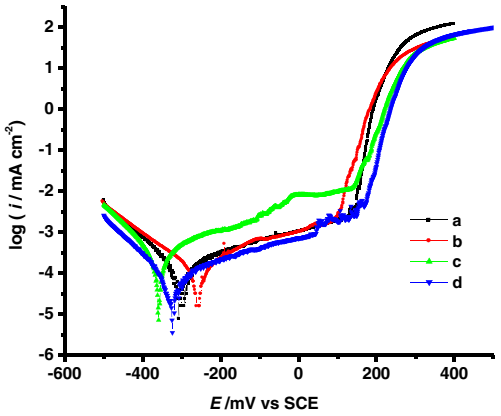


**Fig. 5** Potentiodynamic curves in 0.1 M NaCl for the composite coatings: **a** Ni–Co (1:1)/n-$Al_2O_3$ (5 $g dm^{-3}$) 0.13 $cm^2$, pH5; **b** Ni–Co (1:1)/n-$Al_2O_3$ (5 $g dm^{-3}$) 0.13 $cm^2$, pH11; **c** Ni–Co (1:1)/n-$Al_2O_3$ (5 $g dm^{-3}$) 0.28 $cm^2$, pH5; **d** Ni–Co (1:1)/n-$Al_2O_3$ (5 $g dm^{-3}$) 0.28 $cm^2$, pH 11. Scan rate 0.5 $mV s^{-1}$; 25 °C

For all deposited samples, their corrosion current, $j_{corr}$, shifted to lower values when compared with a Ni pure standard (99.99 %) (Fig. 4). It is obvious that the resistance of Ni–Co films to the attack of chloride ions is determined predominantly by presence and the concentration of Co ions in the bath.

The smallest values of the $j_{corr}$ were obtained for the Ni–Co alloys deposited from an electrolyte containing $Ni^{2+}/Co^{2+}$ in ratio of 1:1 and 10 $g dm^{-3}$ alumina particles. The $j_{corr}$ has practically the same value for the composites obtained from a solution containing $Ni^{2+}/Co^{2+}$ in a ratio of 3:1. Furthermore, it deviated with a maximum of ±0.3 $\mu A/cm^2$ from this value for the layers obtained in the other experimental conditions (Table 3).

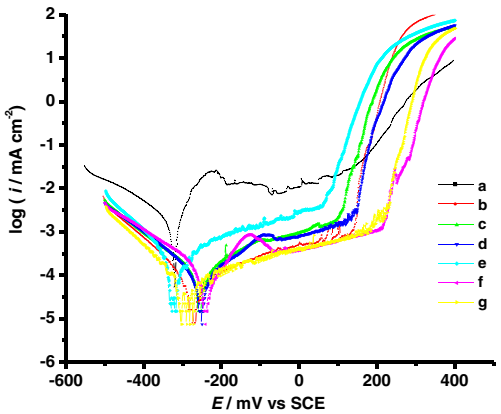


**Fig. 6** Potentiodynamic curves in 0.1 M NaCl for Ni–Co alloys and Ni–Co/n-$Al_2O_3$ composite coatings with 0.13 $cm^2$ surface area: **a** pure Ni; **b** Ni–Co (1:1); **c** Ni–Co (1:1)/n-$Al_2O_3$ (5 $g dm^{-3}$); **d** Ni–Co (1:1)/n-$Al_2O_3$ (10 $g dm^{-3}$); **e** Ni–Co (3:1); **f** Ni–Co (3:1)/n-$Al_2O_3$ (5 $g dm^{-3}$); **g** Ni–Co (3:1)/n-$Al_2O_3$ (10 $g dm^{-3}$). Scan rate 0.5 $mV s^{-1}$; 25 °C

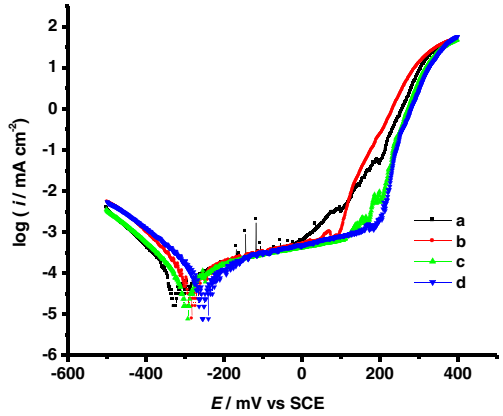


**Fig. 7** Variations in the potentiodynamic curves in 0.1 M NaCl for Ni–Co/n-$Al_2O_3$ (5 $gdm^{-3}$) composite coatings: **a** initial; **b** after 1 day; **c** after 3 days; **d** after 5 days. Scan rate 0.5 $mVs^{-1}$; 25 °C

Comparing all the data obtained in the potentiodynamic polarization experiments (Fig. 5, 6, and 7), one can observe that quite a larger variation in the value of $j_{corr}$ was obtained when changing the alumina concentration in the electrolyte that contained $Ni^{2+}/Co^{2+}$ of 1:1. This fact can be explained by increasing the amount of Co in the alloy. As electrodeposited Co can have hexagonal and cubic structure, while the Ni presents just cubic structure, the increase of Co in the alloy can induce structural changes of the deposited layers, and thus, it can influence the morphology and the corrosion properties of these layers. In this study, the Ni–Co alloys prepared by electrodeposition grow preferentially along the (200) crystalline plane. The Ni–Co/n-$Al_2O_3$ films grow preferential along the (111) plane (XRD data not shown).

The linear polarization experiments show a change of mechanism (from activation controlled to diffusion controlled) already at very close potentials to the OCP values. This fact indicates that the material is very susceptible to pitting in an oxidizing environment that contains also $Cl^-$, even at potentials very closed to the OCP. In the anodic potential region from the potentiodynamic polarization experiments, one can detect the passivation of the Ni–Co and Ni–Co/n-$Al_2O_3$ films.

Most of the samples containing alumina particles exhibit a decrease in the corrosion current recorded at a given potential. This demonstrates that including the alumina particles in the Ni–Co matrix improved the resistance against corrosion of these layers in a 0.1 M NaCl solution. Similar results were obtained when the deposited layers were immersed in a 3.5-wt% $Na_2SO_4$: the resistance against corrosion increased with the increasing concentration of $Al_2O_3$ in the films (not shown).

The effect of pH on corrosion behavior of the deposited films is shown in Fig. 5. The potentiodynamic curves in 0.1 M NaCl are presented here and one can observe that the corrosion potential, $E_{corr}$, shifts to more negative values with the decreasing pH value and with the increasing area of the electrode exposed to the corrosion tests. An increase of pH can thus lead to an increase of the resistance against corrosion of the layers (Fig. 5).

There is an optimum pH value (pH5) at which the formation of corrosion products reaches a maximum. At pH11, the resulting corrosion products are more soluble (Fig. 5)—a fact proven by the higher amount of metal ions detected in the 0.1 M NaCl solution having a pH of 11, after the corrosion tests, when compared with the solutions having a pH of 5 (not shown). The corrosion current is relatively higher for the composite coatings obtained from a bath containing 5 $gdm^{-3}$ $Al_2O_3$ than that for the coatings obtained from a bath containing 10 $gdm^{-3}$ of $Al_2O_3$ nanoparticles, when $Ni^{2+}/Co^{2+}$ ratio in the electrolyte was 1:1 (Fig. 5 and Table 3).

The pitting corrosion is a localized type of corrosion, which implies usually a complex mechanism. Therefore, one cannot apply extrapolation techniques, like Stern–Geary equation or Tafel, in order to get corrosion rates or corrosion resistance values. Therefore, with respect to this, our results can hardly be compared to other reports from literature that did not imply a pitting corrosion [23].

In Fig. 7, one can see the evolution in time of corrosion behavior of the deposited layers, after their immersion in aggressive NaCl solution. It is important to distinguish the corrosion behavior of Ni–Co alloys at short- and long-term exposures in chloride-containing electrolytes. One can see in Figs. 4 and 6 that the layers containing Co all presented a higher resistance against corrosion than the pure Ni standard. The corrosion potential shifted to more anodic values

**Table 3** Electrochemical parameters obtained from polarization curves

| Samples | $Ni^{2+}/Co^{2+}$ ratio in electrolyte | $Al_2O_3$ in electrolyte ($gdm^{-3}$) | $-E_{corr}$ (mV) | $j_{corr}$ ($\mu A/cm^2$) |
|---|---|---|---|---|
| Ni–Co alloys | 3:1 | – | 276 | 0.653 |
| | 1:1 | – | 234 | 0.633 |
| Ni–Co/n - $Al_2O_3$ composite coatings | 3:1 | 5 | 257 | 0.624 |
| | | 10 | 261 | 0.625 |
| | 1:1 | 5 | 292 | 0.646 |
| | | 10 | 330 | 0.612 |

with increasing the time of exposure to the corrosive media of a given sample. This indicates that the deposits corrode the strongest immediately after they are immersed in the NaCl solution, and that the rate of corrosion is consecutively diminished in time. The deposits thus tend to form a passivation layer, and as a final effect, the corrosion potential decreases with ca. 85 mV within 5 days.

## Conclusions

Co–Ni and Co–Ni/n-$Al_2O_3$ electrodeposits were obtained from a Watts-type electrolyte, with different ratio of $Ni^{2+}$/$Co^{2+}$ concentration and different amounts of alumina particles in electrolyte. The composition of the deposited alloys depended on the composition of the electrolyte.

The deposit morphology varied with bath composition and electrodeposition parameters. More homogeneous, fine-grained deposits could be obtained by increasing the $Ni^{2+}/Co^{2+}$ ratio in electrolyte. Electrochemical corrosion experiments and SEM analyses revealed that the corrosion behavior of the deposits is strongly influenced by the content of Co in the alloy.

The electrochemical data from the corrosion examination of Ni–Co and Ni–Co/n-$Al_2O_3$ alloys carried out in 0.1 M NaCl solution (pH5) may be summarized as follows:

- The OCPs of Ni–Co alloys were almost similar as that of pure Ni, but they shifted towards more anodic values when nanoparticles were embedded in the alloy matrix.
- The corrosion current, $j_{corr}$, recorded for both types of coatings (with or without alumina particles) tend to decrease with an increase in the content of Co, and it was all the time lower than that of the Ni standard.
- The corrosion current density decreased more for Ni–Co composite films obtained from a bath with 10 $g dm^{-3}$ alumina than for those obtained from a 5 $g dm^{-3}$ alumina. This demonstrates the formation of a layer which is more resistant against the corrosion and it can also be also attributed to the existence of different ratio of anodic–cathodic corrosion sites for different areas exposed to the test solution for the corrosion.
- From the SEM images of the layers after their exposure to the corrosion solution, one can deduce that the dissolution of metals by corrosion was mixed controlled.

The surface analysis showed that the nano-alumina particles embedded into Ni–Co matrix affect the microstructure and the morphology of the coatings. Thus, the composites had relatively small grain sizes, but, despite this, they did not present a higher resistance against corrosion in 0.1 M NaCl, when compared with Ni–Co alloys.

**Acknowledgments** GC thanks Prof. S. Steinhauser and Prof. T. Lampke, from the Chemnitz University of Technology (Germany), and Mrs. G. Tauchmann and Mrs. E. Benedix for their devoting help. Additionally, the authors would like to thank the colleagues from the Dresden University of Technology (Germany), Institute of Physical Chemistry and Electrochemistry (especially to Prof. W. Plieth) for the permanent support and the fruitful discussions during more than 10 years of collaborations.

This article is dedicated to Professor Walfried Plieth to his 75th birthday. GC had the honor to be accepted to join the group of Prof. Plieth in the TU Dresden within several research stays. The first visit was in 1998, financially supported by a Tempus grant. Many years before Romania became EU member, I had the opportunity to go to Germany in the group of Prof. Plieth and to measure SEM and EDX. I am deeply grateful and I would like to thank very much Prof. Plieth for the opportunity he gave me. Due to him, we had the great chance to develop collaborative work in following years with the electrochemistry group from Dresden University of Technology. Some of my PhD and undergraduate students and some faculty members of Galati University were also visiting scientist in Dresden University of Technology. A Socrates-Erasmus mobility was initiated between our Universities in 2000.

## References

1. Sudhakar P, Daniel BSS, Jeevanandam P (2011) Synthesis of nanocrystalline Co–Ni alloys by precursor approach and studies on their magnetic properties. J Magn Magn Mater 323(17):2271–2280
2. Qin L, Lian J, Jiang Q (2010) Enhanced ductility of high-strength electrodeposited nanocrystalline Ni–Co alloy with fine grain size. J Alloys Compd 504(1):S439–S442
3. Golodnitsky D, Rosenberg Y, Ulus A (2002) Role of anion additives in the electrodeposition of Ni-Co alloy from sulfamate electrolyte. Electrochim Acta 47:2707–2714
4. Kim D, Park DY, Yoo BY, Sumodjo PTA, Myung NV (2003) Magnetic properties of nanocrystalline iron group thin film alloys electrodeposited from sulfate and chloride baths. Electrochim Acta 48:819–830
5. Zhan J, He YH, Zhou DF, Zhang CF (2011) Thermodynamic analysis on synthesis of fibrous Ni-Co alloys precursor and Ni/Co ratio control. Trans Nonferrous Met Soc China 21(5):1141–1148
6. Chang LM, An MZ, Guo HF, Shi SY (2006) Microstructure and properties of Ni-Co/nano-$Al_2O_3$ composite coatings by pulse reversal current electrodeposition. Appl Surf Sci 253(4):2132–2137
7. Chung CK, Chang WT (2009) Effect of pulse frequency and current density on anomalous composition and nanomechanical property of electrodeposited Ni–Co films. Thin Solid Films 517 (17):4800–4804
8. Abd El-Halim M (1984) On the anomalous phenomenon of Co-Ni alloy electrodeposition. Surf Technol 23(3):207–213
9. Arenas JV, Treeratanaphitak T, Pritzker M (2012) Formation of Co–Ni alloy coatings under direct current, pulse current and pulse-reverse plating conditions. Electrochim Acta 62(15):63–72
10. Chonglun F, Piron DL (1996) Study of anomalous nickel-cobalt electrodeposition with different electrolytes and current densities. Electrochim Acta 41(10):1713–1719
11. Vijh AK (1986) Perspective in electrochemical physics. In: Bockris JO'M, Conway BE, White RE (eds) Modern aspects of electrochemistry, vol 17. Plenum, New York
12. Di Bari GA (2000) Nickel alloys, cobalt and cobalt alloys. In: Schlesinger M, Paunovic M (eds) Modern electroplating, 4th edn. Wiley, New York, pp 561–564, Chapter 13

13. Chang LM, Guo HF, An MZ (2008) Electrodeposition of Ni–Co/$Al_2O_3$ composite coating by pulse reverse method under ultrasonic condition. Mater Lett 62:3313–3315
14. Oh ST, Sando M, Niihara K (2001) Mechanical and magnetic properties of Ni-Co dispersed $Al_2O_3$ nanocomposites. J Mater Sci 36:1817–1821
15. Chang LM, An MZ, Shi SY (2006) Microstructure and characterization of Ni-Co/$Al_2O_3$ composite coatings by pulse reversal electrodeposit. Mater Chem Phys 100(2–3):395–399
16. Dietrich D, Scharf I, Nickel D, Shi L, Grund T, Lampke T (2011) Ultrasound technique as a tool for high-rate incorporation of $Al_2O_3$ in NiCo layers. J Solid State Electrochem 15:1041–1048
17. Tian BR, Cheng YF (2007) Electrolytic deposition of Ni-Co-$Al_2O_3$ composite coating on pipe steel for corrosion/erosion resistance in oil sand slurry. Electrochim Acta 53(2):511–517
18. Srivastava M, Srinivasan A, William Grips VK (2011) Influence of zirconia incorporation on the mechanical and chemical properties of Ni-Co alloys. Amer J Mater Sci 1(2):113–122
19. Pané S, Gómez E, García-Amorós J, Velasco D, Vallés E (2007) First stages of barium ferrite microparticles entrapment in the electrodeposition of CoNi films. J Electroanal Chem 1:41–47
20. Gómez E, Ramirez J, Vallés E (1998) Electrodeposition of Co-Ni alloys. J Appl Electrochem 28:71–79
21. Bo Y, Hwang E, Scherson DA (1996) In situ quartz crystal microbalance studies of nickel hydrous oxide films in alkaline electrolytes. J Electrochem Soc 143:37–43
22. Qiao G, Jing T, Wang N, Gao Y, Zhao X, Zhou J, Wang W (2005) High-speed jet electrodeposition and microstructure of nanocrystalline Ni–Co alloys. Electrochim Acta 50:85–92
23. Ciubotariu AC, Benea L, Lakatos Varsanyi M, Dragan V (2008) Electrochemical impedance spectroscopy and corrosion behaviour of $Al_2O_3$-Ni nano composite coatings. Electrochim Acta 53:4557–4563
24. Brenner A (1963) Electrodeposition of alloys, principles and practice. Academic, New York
25. Revie RW, Uhlig HH (2008) Corrosion and corrosion control. An introduction to corrosion science and engineering, 4th edn. Wiley, New Jersey
26. Frankel GS (1998) Pitting corrosion of metals. A review of the critical factors. J Electrochem Soc 145:2186–2198
27. Kaesche H (2011) Die Korrosion der Metalle. Physikalisch-chemische Prinzipien und Aktuelle Probleme, 3rd edn. Springer, Heidelberg